Energy Islands – Floating LiDAR Measurements

Motion correction of turbulence intensity. WP3: Baltic Sea pre-deployment verification tests

C75486-TI1-R-02 03 | 20 March 2024
Final
ENERGINET

Document Control

Document Information

Project Title	Energy Islands – Floating LiDAR Measurements
Document Title	Motion correction of turbulence intensity. WP3: Baltic Sea pre-deployment verification tests
Fugro Project No.	C75486
Fugro Document No.	C75486-TI1-R-02
Issue Number	03
Issue Status	Final

Client Information

Client	ENERGINET
Client Address	ENERGINET Eltransmission A/S, Tonne Kjærsvej 65, DK-7000 Fredericia, Denmark
Client Contact	Guillaume Mougin, Kim Parsberg Jakobsen and Gry Schachtschabel

Revision History

Issue	Date	Status	Comments on Content	Prepared By	Checked By	Approved By
01	17 August 2023	Draft	First issue	Felix Kelberlau		
02	04 December 2023	Draft	Second Issue	Felix Kelberlau	Irene Pathirana	
03	20 March 2024	Final	Final Issue	Irene Pathirana	Irene Pathirana	Arve Berg

Contents

Figures

Tables

Abbreviations

Abbreviation	Definition
CFARS	Consortium for Advancing Remote Sensing
comp.	Motion compensated
CW	Continuous wave
FLS	Floating LiDAR system
IMU	Inertial measurement unit
KPI	Key performance indicator
LiDAR	Light detection and ranging
MBE	Mean bias error
MRU	Motion reference unit
MSL	Mean sea level
NaN	Not-a-number
PDV	Pre-deployment verification
RLL	Reference Land LiDAR
RMSE	Root mean square error
Roadmap	Carbon Trust Offshore Wind Accelerator Roadmap
RTO	Regression through origin, single-variant regression
SWLB	Seawatch Wind LiDAR Buoy
TI	Turbulence intensity
uncomp.	Not motion compensated (uncompensated)
UTC	Universal time coordinated
VAD	Velocity–azimuth display

Conventions

Convention	Description
Directions	Directions are given in degrees (◦) increasing clockwise from North. The direction is defined as incoming: 0◦ meanswind blowing from North, 90◦ from East etc. Directions are relative to true north.
Turbulence intensity	Turbulence intensity is defined as the standard deviation of horizontal wind velocity fluctuations divided by the horizontalmean wind velocity during 10-minute long averaging intervals.
Time	All times are UTC and timestamps mean the beginning of an averaging interval.

1. Introduction

Estimates of turbulence intensity (TI) from floating LiDAR systems (FLS) are influenced by motion. Rotational and translational motion in all six degrees-of-freedom leads to an overestimation of TI measured by an FLS when compared to values acquired by a collocated fixed LiDAR system of the same type. Energinet has asked Fugro to correct the TI measurements from the SEAWATCH Wind LiDAR Buoys (SWLB) deployed in the Baltic Sea for buoy motions. The correction of measured TI for buoy motions is split in two (2) work packages:

- WP3: Correction of TI measured during PDV (this report).
- WP4: Correction of TI measured during campaign.

This report describes two comparisons of FLS measurement data against fixed reference LiDARs.

1. SWLB data from WS199 deployed at Frøya against a fixed ZX 300 LiDAR [1]; and
2. SWLB data from SWLB044 deployed at Frøya against a fixed ZX 300 LiDAR [2].

The ZX 300 used on the buoys and onshore at Frøya are continuous-wave (CW) velocity-azimuth-display (VAD) scanning profiling wind LiDARs. For both comparisons, three datasets are available that constitute the data basis of this report:

- Reference land LiDAR (RLL) data
- FLS data, uncompensated
- FLS data, motion-compensated

Table 1.1 gives information about the LiDAR units used during both pre-deployment verification (PDV) trials.

System	Location	LiDAR unit	Firmware
RLL	Frøya (fixed)	428	v2.202
FLS1	WS199	898	v2.202
FLS2	SWLB044	993	v2.2029

Table 1.1: Details of LiDAR units

1.1 Guidelines for assessment of turbulence intensity

The Offshore Wind Accelerator Roadmap (Roadmap) [3] is a widely accepted guidance document that suggests methods and key performance indicators (KPIs) including acceptance thresholds for FLS unit verifications. Unfortunately, this accounts only for the assessment of primary wind data, i.e., 10-minute average wind speed and direction. For secondary wind data, like TI, the Roadmap does not prescribe any acceptance criteria. Instead, it only recommends measuring TI and compare it to measurements from a trusted reference source. It then details that a comparison against conventional (i.e., in-situ) anemometry is recommended. For the comparison it defines the slope of single variant regression, i.e., linear regression through the origin (RTO) as the first KPI and its correlation co-efficient as the second KPI. Due to the weaknesses of the suggested KPIs, detailed in [4], we do not use them in this report.

Instead, the CFARS Site Suitability Initiative [5] can be seen as a first guidance document for the assessment of TI estimates from FLS. It suggests using the Mean Bias Error (MBE) for each 1m/s-wide wind speed bin i

$$MBE_i = \frac{1}{N_i}\sum_{n=1}^{N_i}(TI_{comp,n,i} - TI_{ref,n,i})$$

where TI_{comp} is the comparison quantity (TI_{FLS}), TI_{ref} is the reference quantity (TI_{RLL}), N_i is the number of values in wind speed bin i, and n is the individual datapoint. In addition to the MBE as an estimator of accuracy, the Root Mean Square Error (RMSE) shall be used to measure the TI precision. It is calculated according to

$$RMSE_i = \sqrt{\frac{1}{N_i}\sum_{n=1}^{N_i}(TI_{comp,n,i} - TI_{ref,n,i})^2}$$

Furthermore, CFARS suggests using representative TI in comparisons. Representative TI is defined as the 90th percentile of a TI distribution. It is calculated from $TI_{mean,i}$, the mean of all TI values in a bin and $TI_{std,i}$, its standard deviation by

$$TI_{Rep,i} = TI_{mean,i} + 1.28TI_{std,i}$$

The representative TI error being the difference between the representative TI from FLS and RLL. In this report we will use MBE, representative TI error and RMSE as primary benchmark criteria.

Plots of the benchmark data will show which velocity bins are significant according to the following criteria:

$$n_i > \frac{N}{2n_b},$$

where $n_b$is the number of bins, N the total number of data points, and $n_i$the number of data points in bin i. And

$$\frac{\sigma(d_i)}{\sqrt{n_i}}\frac{V_{ref,i}}{100} < 0.03m/s,$$

where $d_i$is the data in bin i, $\sigma(d_i)$ the standard deviation of data in bin i, and $V_{ref,i}$ the mean value of the reference wind speed in bin i. These significance criteria are adopted from Eqs. L.2 and L.3 of IEC [6].

2. Instrumentation and measurement configuration

2.1 Summary of instrumentation and measurement scheme

Buoys WS199 and SWLB044 were used for the data acquisition during the pre-deployment validations reported in this document. These two SWLB buoys are not optimized for deriving motion-compensated estimates of turbulence intensity, as neither line-of-sight velocities[1] from the LiDAR are recorded, nor velocity data from surge and sway directions are available.

The measurement platform of the FLS is a SEAWATCH Wind LiDAR Buoy based on the original SEAWATCH Wavescan Buoy design. The wind LiDAR used in this project is the marinized version of the ZX 300 LiDAR type (units 898 and 993) including their Airmar 200 meteorological station positioned on the mast of the buoys.

To estimate wave statistics, the buoys are equipped with an inertial measurement unit (IMU). This IMU is part of the Wavesense wave sensor. Its software is optimized for computations in the frequency domain. It is set up to generate and store bursts of 2048 samples with 2 Hz frequency every ten minutes. These bursts of motion data are available for the four degrees of freedom pitch, roll, yaw, and heave. Surge and sway data are not available with the used configuration.

Furthermore, accurate heading data is acquired by a Septentrio DualGPS system. The GPS system outputs timestamped yaw and pitch data with a frequency of 1 Hz. It is used to assign accurate timestamps to the Wavesense motion data.

2.2 LiDAR measurement principle

The SWLB is equipped with a ZX 300M continuous-wave (CW) profiling wind LiDAR that can measure wind velocities remotely. The LiDAR continuously emits an infrared laser beam. The beam is deflected from the zenith by the half-cone opening angle (30.6°) and rotates around the zenith with a continuously changing azimuth angle. In this way, the laser beam illuminates a measurement cone during each full beam rotation.

By determining the Doppler shift of radiation that is backscattered into the direction of the laser source, the LiDAR device can determine the radial velocity of particles and aerosols that are moving with the speed of the wind. One full rotation along the measurement cone takes one second. All radial velocities determined during this period are then processed to reconstruct one three-dimensional wind vector.

During each of these scanning cycles, optical focusing concentrates the laser radiation onto one desired measurement elevation above the LiDAR and several elevations can be scanned consecutively after refocusing. The LiDAR on the SWLB is configured to scan a total of 11

[1] VAD scanning profiling wind lidar reconstruct three-dimensional wind vectors from at least 3 (49 in the case of the ZX 300) radial velocity samples measured along the laser beam (i.e., line-of-sight velocities). The lidars used on WS199 and SWLB044 measure these line-of-sight velocities as intermediate values but do not record them. This is one of the reasons that make it impossible to correct the TI estimates in the way that Fugro uses for other projects.

elevations which takes approx. 17 seconds. As a result, approx. 36 samples from each measurement elevation can be taken during an averaging period of 10 minutes length.

Horizontal homogeneity of the wind field is an underlying assumption of the wind vector reconstruction process, i.e., the estimated wind vectors are only representative for the real wind conditions if the wind velocity is constant at all positions along the measurement cone. For mean wind speed and direction, it is sufficient that the wind field is homogeneous in the mean. In non-complex terrain (like offshore) this requirement is usually fulfilled.

For correct measurements of turbulence intensity (TI), the wind field above the LiDAR would need to be constant at all times. By definition, this is not the case in turbulent flow. Also, the non-zero averaging length along the laser beam that increases with measurement height and the limited sampling frequency lead to systematic measurement errors and increase the uncertainty of TI measurements from profiling wind LiDAR [7].

2.3 Motion-compensation of turbulence intensity values

Measurements of turbulence intensity with a profiling CW wind LiDAR from a moving platform like the SWLB are influenced by platform motion. The influence of motion is dependent on the amplitude and frequency of the motion in all six degrees of freedom as well as the prevailing wind conditions. For being able to estimate TI with an accuracy similar to measurements from a fixed LiDAR device of the same type, motion compensation must be applied. In cooperation with the Norwegian University of Science and Technology (NTNU), Fugro developed and validated a method to measure and remove the effect of motion from the measurements [8]. This method cannot be applied for the available buoy data as the LiDAR line-of-sight velocities have not been recorded, and the timestamps of the motion data are not sufficiently accurate. Furthermore, no motion data in surge and sway degrees of freedom are available. Instead, a modified methodology for motion correction had to be developed and tested. In the following, we will describe the data processing performed on the available data from buoys WS199 and SWLB044:

- lidar1hz files: Unaveraged LiDAR data sampled via MODBUS
- PFF data: Wavesense motion data
- sept*__SBF_AttEuler1.txt files: Septentrio motion data

These data are not transmitted by satellite communication but are downloaded from the buoys during service visits or after recovery. The data is then post-processed to calculate motion-compensated wind data. The data processing consists of the following steps:

1. Assign accurate timestamps to Wavesense motion data by synchronization with DGPS yaw and pitch data
2. Find correct timing of first beam of each velocity-azimuth display (VAD) scan

3. Calculate 10-minute mean wind speed and direction including 180 deg ambiguity correction
4. Generate synthetic line-of-sight data from known beam geometry, timing and mean wind data, without turbulence
5. Perturbate synthetic line-of-sight data using motion data for a series of possible temporal offsets between LiDAR and motion timing
6. Reconstruct three-dimensional wind vectors from the synthetic motion-perturbed line-of-sight data
7. Subtract wind speed fluctuations of the synthetic wind vector data from the lidar1hz data and find temporal offset with the lowest resulting wind speed variance
8. Calculate the standard deviation of horizontal wind speed fluctuations by subtracting the motion-perturbed values from the measured values, assuming that they are statistically uncorrelated
9. Average TI reduction over all measurement elevations and one hour to smoothen the motion-compensated TI results

Estimates of motion-compensated turbulence intensity on a 10-minute level (i.e., TI values) are the main output of the described method. These values can be processed as if they were acquired by a fixed LiDAR unit. Still, it should be noted that the uncertainty is higher than if the values were produced with the method described in [8]. For best TI estimates, it is recommended that future measurement campaigns will be performed with new or upgraded SWLB that measure timestamped motion data in six degrees of freedom and record LiDAR line-of-sight velocities.

3. Data handling

3.1 Data file description

Files: *WS199atFroya_data.csv*
SWLB044atFroya_data.csv

These files contain mean wind speed as measured by the reference LiDAR (U_RLL), TI data from the fixed reference LiDAR (TI_RLL), mean wind speed data as calculated by the internal data processing of the floating LiDAR (U_FLS_ZPH), TI estimates without motion compensation (TI_FLS_unc) and with motion compensation (TI_FLS_com). For each of these values one data column represents data from one measurement elevation. Ten numbered columns represent the ten comparable measurement elevations at the Frøya test site, 40, 60, 80, 100, 120, 140, 160, 180, 200 and 250 meters above mean sea level.

3.2 Data filtering

For the data comparisons, we exclude data that is filtered by either the reference LiDAR or the FLS and remove data from intervals during which the mean wind speed measured by the reference LiDAR was lower than 2 m/s. The motivation to apply this low wind speed filter is that, first, very low wind speeds are of low importance for wind site assessment, and second, data quality is known to be low at very low wind speeds. No other filters were applied to the data presented in this report. All filtered values are marked as “NaN” in the data files.

4. Results

In the following, PDV results are presented and interpreted. Within each subsection, we first report the results of WS199 at Frøya and then SWLB044 at Frøya. For the assessment, we use the KPIs introduced in Section 1.1.

4.1 Mean bias error

Figures 4.1 and 4.2 show the mean bias error of TI estimates from the FLS with and without motion compensation based on data from the deployment of WS199 and SWLB044 at the Frøya test site, respectively. The MBE is binned by 1m/s wide velocity bins with significant and insignificant bins indicated by filled and unfilled markers, respectively. As significance criteria we adopted the guidance given in Eqs. L.2 and L.3 of IEC [6].

Overall, the MBE results of TI data from WS199 show that the applied method for motion compensation works well because motion-induced TI is reduced for all velocity bins and all measurement elevations. Most MBE values for motion-compensated data are reasonably close to zero. The largest deviations are observed for the lowest wind speed bin (2…3m/s) for which the MBE is above 2% at all elevations. Also, the second and third lowest wind speed bins (3…4m/s & 4…5m/s) show relatively high MBE values around 1.5%. These values indicate that, despite significant reduction of motion-induced TI, the applied method for motion compensation works worse at low wind speeds. And it must be assumed that the motion-compensated TI data is, to some degree, still affected by buoy motion. The reason for the apparently incomplete motion compensation at low velocities might be the negligence of horizontal translatory motion in the processing. Relatively speaking, translatory motion has a stronger impact at low wind speeds. At the lowest elevation (40m), slightly negative values are found. This has been seen for other trials at the Frøya test site and can be explained by the different elevation of FLS and RLL above sea level and terrain effects, including the sea to land transition. Nearly all other MBE values are positive. This shows that the method is conservative and does not “overcompensate” the effects of motion.

MBE data from SWLB044 shown in Fig. 4.2 show very similar results and all effects described above or WS199 are valid also for SWLB044. The similarity can be explained by the fact that both PDV trials were conducted simultaneously with two FLS of the same type. The resemblance of data demonstrates the robustness of the method.

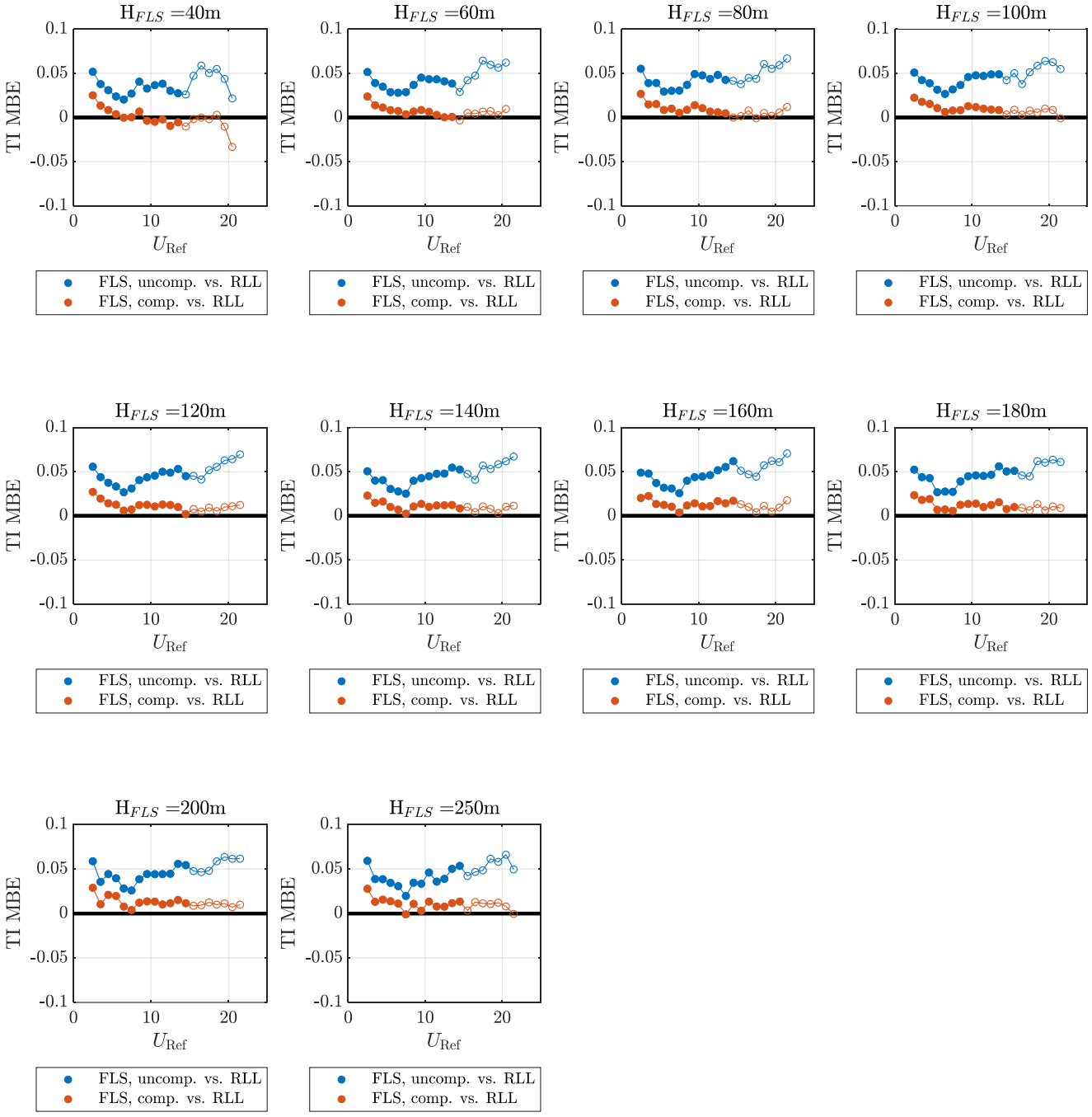

Figure 4.1: Mean bias error (MBE) of TI for data from WS199 at Frøya with (red) and without (blue) motion compensation for all comparable measurement elevations.

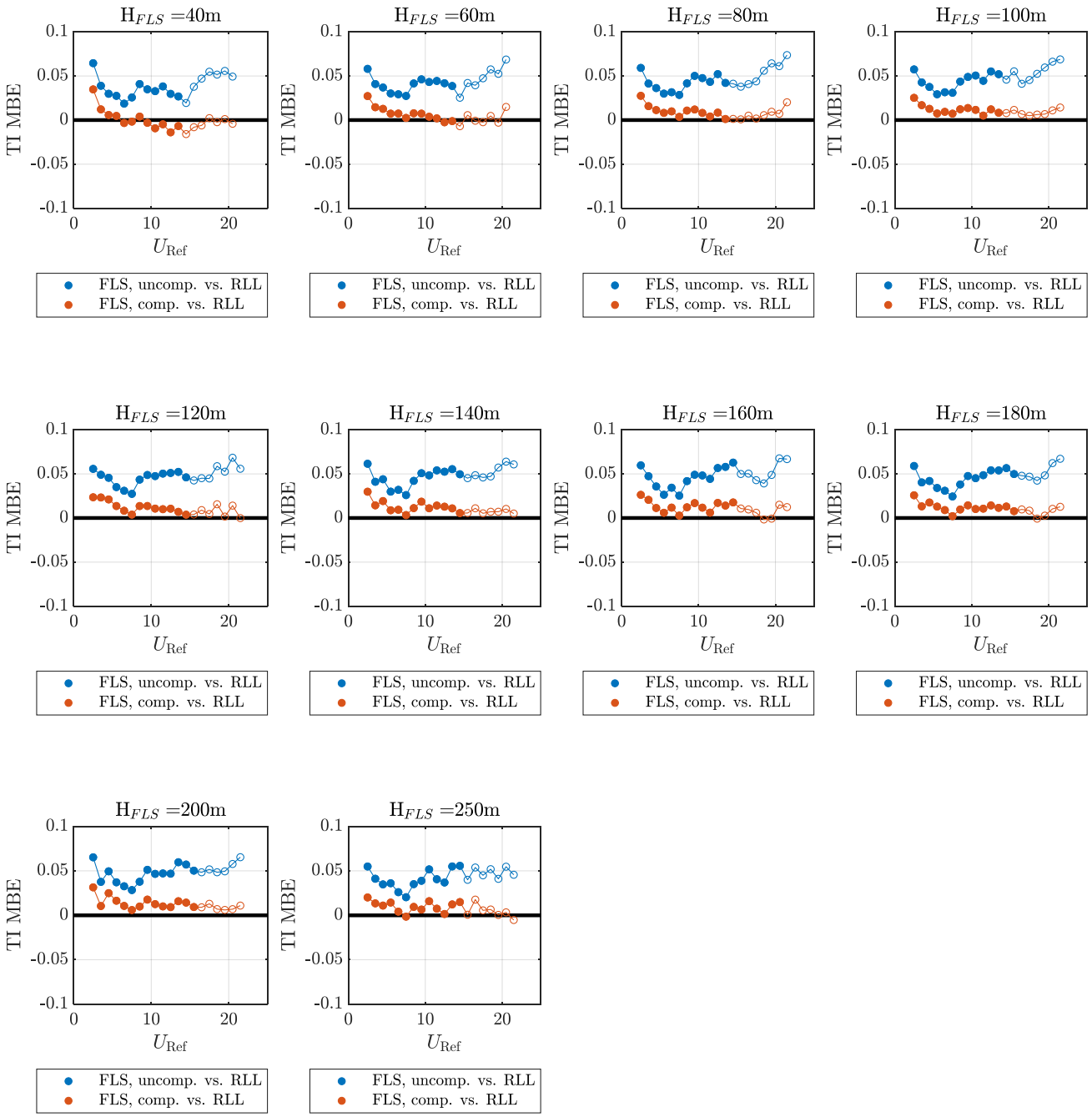

Figure 4.2: Mean bias error (MBE) of TI for data from SWLB044 at the Frøya test site with (red) and without (blue) motion compensation for all comparable measurement elevations.

4.2 Representative TI error

Figures 4.3 and 4.4 show the velocity-binned mean error of representative TI for both buoys. For WS199, the motion-compensated values of representative TI are similar to the representative TI values measured by the RLL. Some scattered strong deviations are present at low wind speed bins (<5m/s) and tendentially at high elevations (>120m). Separate analysis of data within the affected velocity bins has shown the outliers at high elevations can be explained by non-successful cloud detection and removal within the floating ZX 300 LiDAR. When the time series of reconstructed horizontal wind speeds shows fluctuations between measurements corresponding to the desired elevation and the higher elevation of cloud layers, very large TI measurements can be the consequence. With additional filtering, the effect can be mostly removed. No such additional filters have been applied to the data presented here. The large outliers at low wind speeds (e.g., 160m, 3…4m/s) are visible in the plots of both, the uncompensated and compensated data, which indicates that they are not caused by problems in the motion compensation but rather by statistical variation. Despite the large variance in the representative TI error data that comes with some negative values, the results are conservative, i.e., the representative TI error is tendentially slightly positive.

As it was the case for MBE, the results acquired by SWLB044 resemble the data from WS199 (see Fig. 4.2). It can be pointed out that the deviations at low wind speeds and the outliers at high elevations are somewhat larger for SWLB044 than for WS199. If this is not random, it could be explained by the longer separation distance between RLL and SWLB044 (480m) and WS199 (350m), respectively.

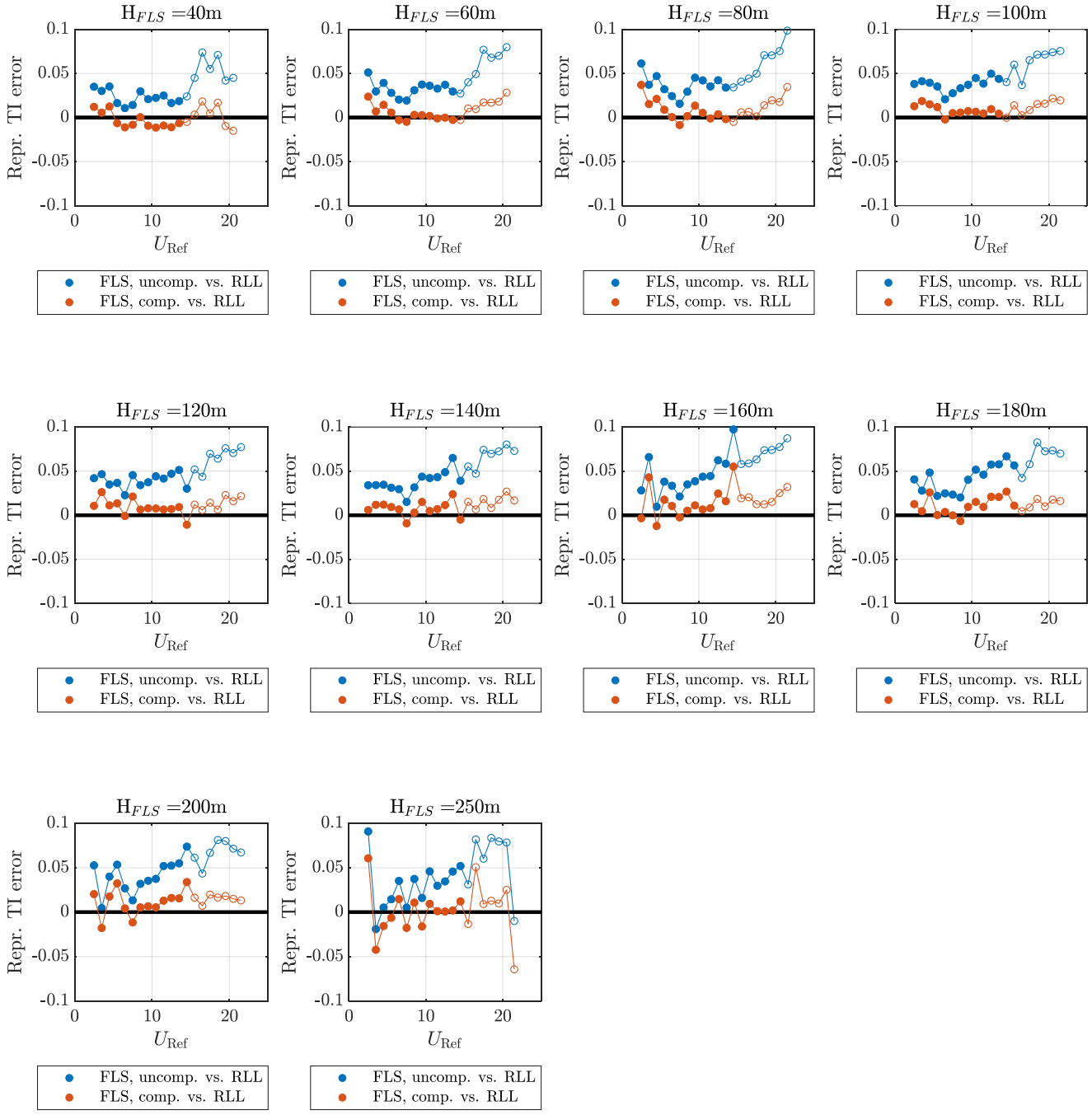

Figure 4.3: Error of representative TI for data from WS199 at Frøya with (red) and without (blue) motion compensation for all comparable measurement elevations.

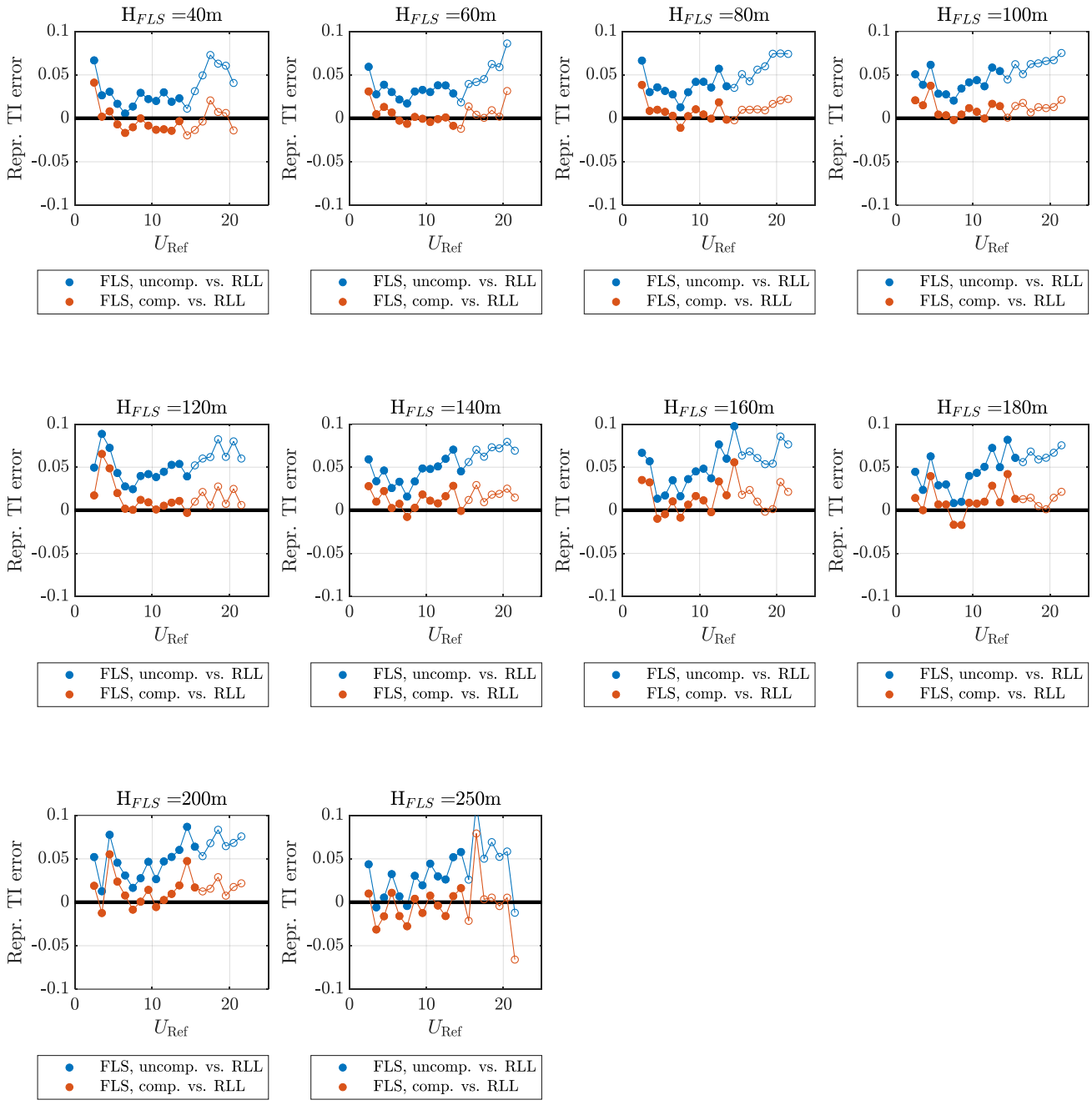

Figure 4.4: Error of representative TI for data from SWLB044 at Frøya with (red) and without (blue) motion compensation for all comparable measurement elevations.

4.3 Root mean square error

While the previous figures quantified the accuracy of motion-compensated FLS TI, Figures 4.5 and 4.6 present RMSE as a measure of precision. Generally speaking, the reduction depends on the velocity with stronger reduction at higher wind speeds. The RMSE values of motion-compensated TI data are the lowest at high wind velocities.

For data from both buoys every RMSE value at each elevation and each velocity bin was reduced by the motion compensation. At low wind speeds, especially at high elevations, the reduction is minimal.

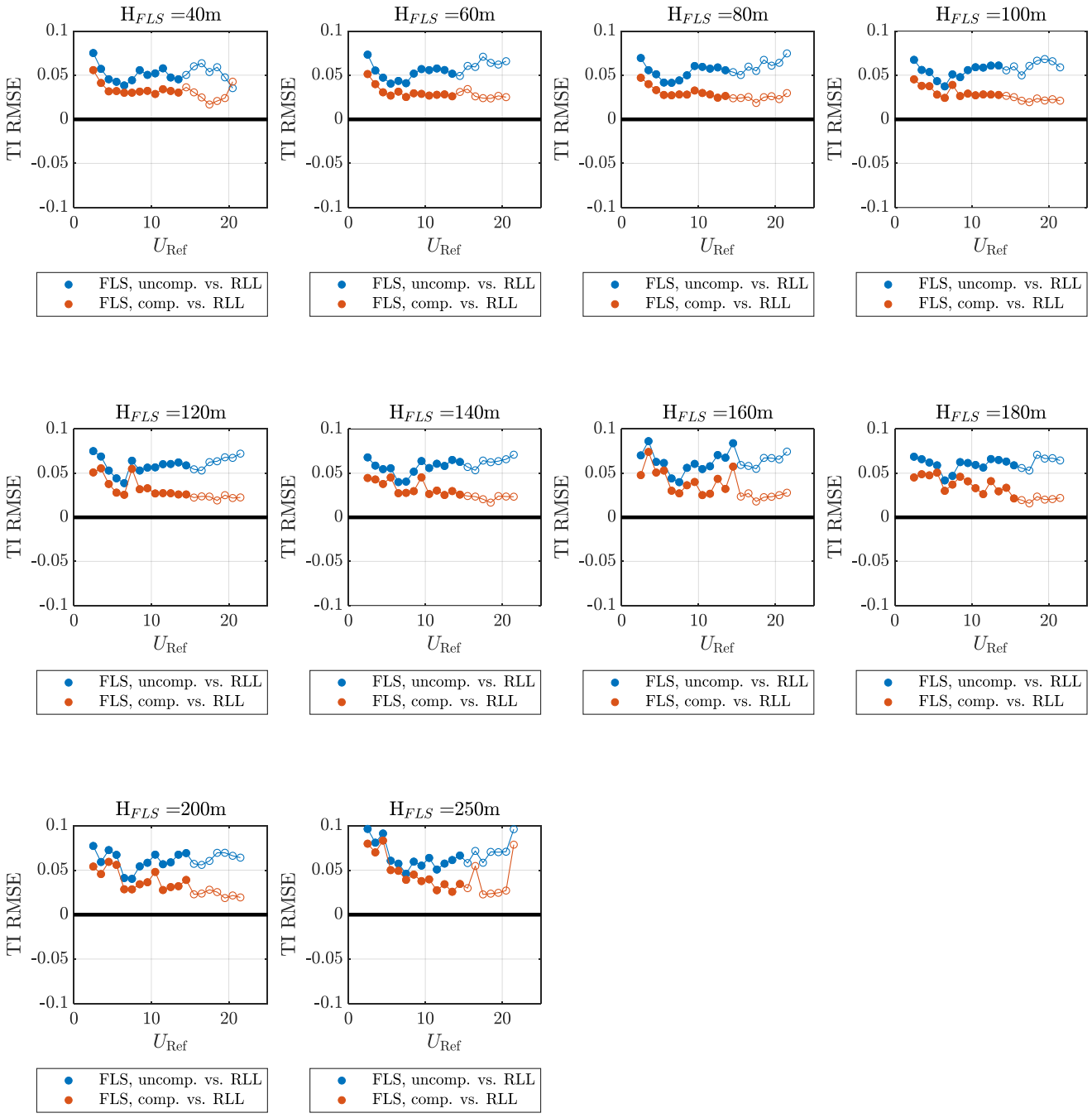

Figure 4.5: Root mean square error (RMSE) of FLS TI for data from WS199 at Frøya with (red) and without (blue) motion compensation for all comparable measurement elevations.

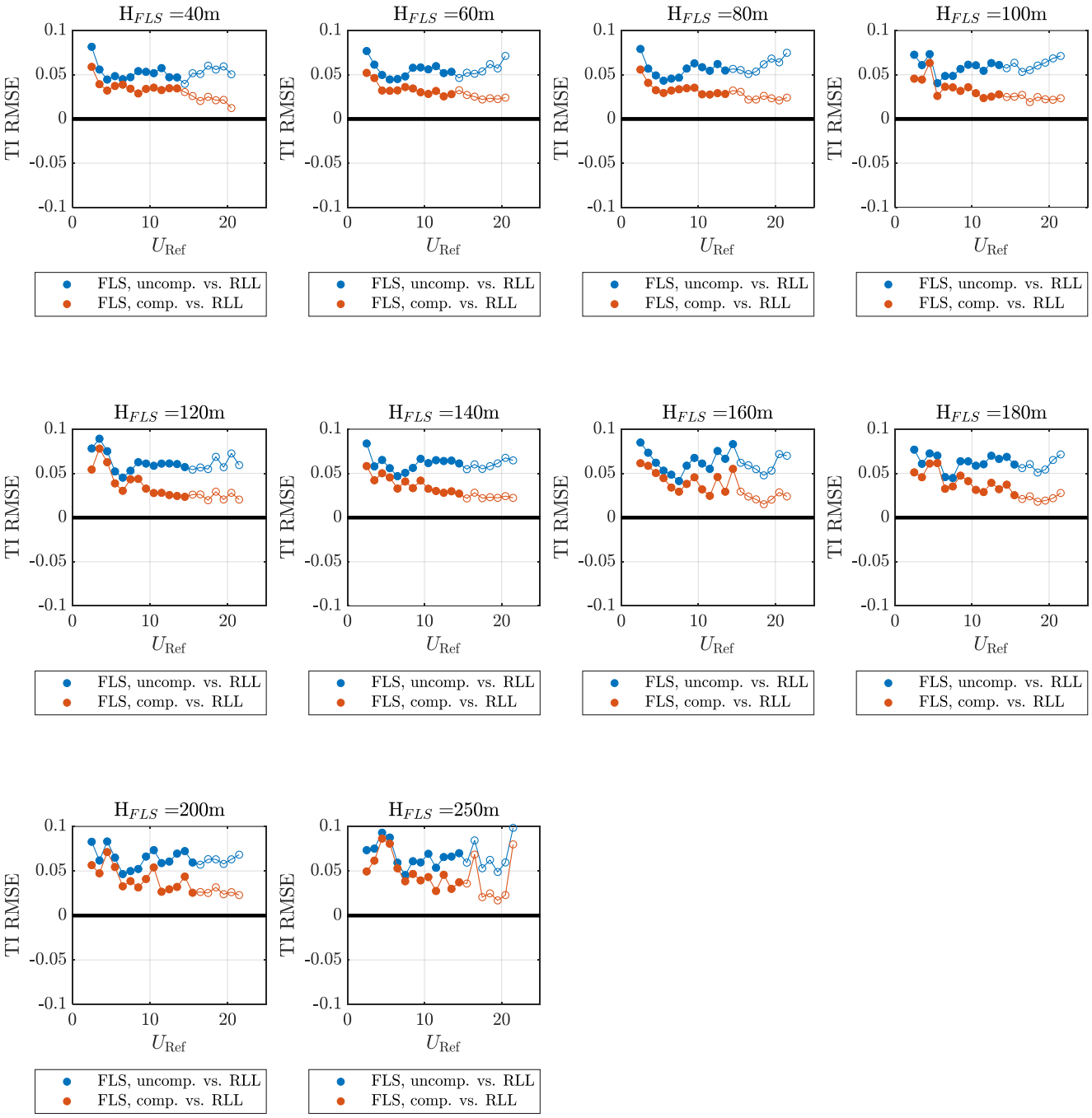

Figure 4.6: Root mean square error (RMSE) of FLS TI for data from SWLB044 at Frøya with (red) and without (blue) motion compensation for all comparable measurement elevations.

5. Conclusion

This report describes the application of a motion compensation algorithm on TI data from two SWLBs during PDVs. SWLB WS199 and SWLB044 have been trialed simultaneously against a fixed ZX300 LiDAR at Fugro's Frøya test site. Data basis for the motion compensation process are the unaveraged reconstructed wind vectors from the floating LiDARs and motion data from the Wavesense instrument as well as the Septentrio DPGS system onboard the FLS. This method has been custom-made for this project.

By the application of the method, most of the motion-induced turbulence intensity could have been removed from the measurements of both FLS. On average, the remaining mean bias of motion-compensated TI data from both buoys is slightly positive. The largest deviations are found at low wind speeds, where the performance of the algorithm appears to be slightly reduced. At high measurement elevations some outliers are found that can be traced back to problems with the cloud detection and removal algorithm of the floating LiDAR which, when not working correctly, can result in too high TI values. Therefore, the deviations are not concerning for the assessment of the motion compensation method.

Results for the representative TI error show that also the distribution of TI values within each wind velocity bin is after motion compensation comparable to the reference data. The RMSE results presented in this report show that motion compensation improves the TI data quality consistently. It is positive that datasets from both buoys show very similar results since this indicates the robustness of the method.

Despite the limited data basis without line-of-sight velocity measurements and incomplete motion data, the method applied for motion compensation of the measured turbulence intensity performs well. The estimated values of turbulence intensity from the SWLBs are significantly closer to values from the fixed reference LiDARs than the uncompensated original values. Therefore, using the compensation method on campaign data is expected to reduce measurement errors induced by buoy motion and provide more accurate turbulence intensity estimates.

6. References

[1] DNV, "WS199 Independent performance verification of Seawatch Wind Lidar Buoy at Frøya, Norway. 10281716-R-11, Rev. A," 2021.

[2] DNV, "SWLB044 Independent performance verification of Seawatch Wind Lidar Buoy at Frøya, Norway. 10281716-R-12, Rev. B," 2021.

[3] OWA, "Carbon Trust Offshore Wind Accelerator Roadmap for the Commercial Acceptance of Floating LiDAR technology. Version 2.0, October 2018," 2018.

[4] F. Kelberlau, V. Neshaug and A. Venu, "Assessment of turbulence intensity estimates from floating lidar," *J. Phys.: Conf. Ser.,* vol. 2507, no. 1, p. 012014, 2023.

[5] CFARS, "Site Suitability Initiative: An Open Source Approach to Evaluate the Performance of Remote Sensing Device (RSD) Turbulence Intensity Measurements & Accelerate Industry Adoption of RSDs for Turbine Suitability Assessment," 2021.

[6] IEC, *61400-12-1:2017 edition 2.0 Wind energy generation systems – power performance measurements of electricity producing wind turbines,* 2017.

[7] F. Kelberlau and J. Mann, "Better turbulence spectra from velocity–azimuth display scanning wind lidar," *Atmospheric Measurement Techniques,* vol. 12, no. 3, p. 1871–1888, 2019.

[8] F. Kelberlau, V. Neshaug, L. Lønseth, T. Bracchi and J. Mann, "Taking the motion out of floating lidar: Turbulence intensity estimates with a continuous-wave wind lidar," *Remote Sensing,* vol. 12, no. 5, 2020.

Appendix A

Tabulated results

A. Tabulated results

Tables 4.1 and 4.2 show the TI error results of the motion-compensated FLS. MBE values with a magnitude beyond ±1% TI are marked yellow and values above ±2% TI are marked red. For representative TI the respective thresholds are ±1.5% and ±3%. For RMSE the definition of a constant threshold does not appear useful due to the higher values at low wind speeds. The calculation of average values in the last column is based on the velocity bins from 4 m/s to 16 m/s and the average values in the last row of each error type is based on the comparable measurement heights excluding the lowest elevation.

Aggregated TI data

Mean bias error (MBE)

Height	Velocity bin [m/s]																				
[m]	2...3	3...4	4...5	5...6	6...7	7...8	8...9	9...10	10...11	11...12	12...13	13...14	14...15	15...16	16...17	17...18	18...19	19...20	20...21	21...22	*4...16*
40	2.5 %	1.4 %	0.8 %	0.4 %	0.0 %	0.0 %	0.7 %	-0.4 %	-0.5 %	-0.2 %	-0.9 %	-0.5 %	-1.0 %	-0.2 %	0.0 %	-0.2 %	0.3 %	-1.0 %	-3.3 %		**-0.1 %**
60	2.4 %	1.4 %	1.1 %	0.8 %	0.7 %	0.4 %	0.7 %	0.8 %	0.6 %	0.3 %	0.0 %	0.1 %	-0.3 %	0.5 %	0.4 %	0.7 %	0.7 %	0.3 %	1.0 %		**0.7 %**
80	2.7 %	1.5 %	1.5 %	0.9 %	1.0 %	0.5 %	0.9 %	1.4 %	1.1 %	0.7 %	0.6 %	0.5 %	0.0 %	0.2 %	0.8 %	-0.1 %	0.5 %	0.2 %	0.6 %	1.2 %	**0.8 %**
100	2.2 %	1.8 %	1.5 %	1.1 %	0.6 %	0.8 %	0.8 %	1.3 %	1.2 %	1.0 %	0.9 %	0.8 %	0.3 %	0.9 %	0.3 %	0.8 %	0.6 %	1.0 %	0.9 %	-0.1 %	**0.9 %**
120	2.7 %	2.0 %	1.4 %	1.3 %	0.6 %	0.7 %	1.2 %	1.3 %	1.1 %	1.3 %	1.2 %	1.0 %	0.2 %	0.8 %	0.5 %	0.9 %	0.5 %	1.0 %	1.1 %	1.2 %	**1.1 %**
140	2.3 %	1.5 %	1.6 %	1.0 %	0.7 %	0.2 %	1.1 %	1.3 %	1.0 %	1.2 %	1.2 %	1.2 %	0.8 %	1.0 %	0.4 %	1.1 %	0.8 %	0.3 %	1.0 %	1.1 %	**1.0 %**
160	2.0 %	2.2 %	1.3 %	1.2 %	1.0 %	0.4 %	1.2 %	1.4 %	1.1 %	1.1 %	1.7 %	1.4 %	1.7 %	1.3 %	1.0 %	0.4 %	1.1 %	0.5 %	0.9 %	1.8 %	**1.2 %**
180	2.3 %	1.8 %	1.9 %	0.7 %	0.7 %	0.6 %	1.2 %	1.4 %	1.4 %	1.0 %	1.2 %	1.5 %	0.8 %	1.0 %	0.9 %	0.6 %	1.3 %	0.6 %	1.1 %	0.9 %	**1.1 %**
200	2.9 %	1.0 %	2.1 %	2.0 %	0.8 %	0.4 %	1.2 %	1.4 %	1.3 %	1.0 %	1.2 %	1.5 %	1.2 %	0.9 %	0.9 %	1.2 %	1.0 %	1.1 %	0.7 %	1.0 %	**1.2 %**
250	2.8 %	1.3 %	1.6 %	1.4 %	1.1 %	-0.1 %	1.1 %	0.3 %	1.3 %	0.8 %	0.8 %	1.2 %	1.3 %	0.3 %	1.3 %	1.1 %	1.1 %	1.2 %	0.8 %	0.0 %	**1.0 %**
...	**2.5 %**	**1.6 %**	**1.5 %**	**1.1 %**	**0.7 %**	**0.4 %**	**1.0 %**	**1.0 %**	**1.0 %**	**0.8 %**	**0.8 %**	**0.9 %**	**0.5 %**	**0.7 %**	**0.7 %**	**0.7 %**	**0.8 %**	**0.5 %**	**0.5 %**	**0.9 %**	**1.0 %**

Representative TI error

Height	Velocity bin [m/s]																				
[m]	2...3	3...4	4...5	5...6	6...7	7...8	8...9	9...10	10...11	11...12	12...13	13...14	14...15	15...16	16...17	17...18	18...19	19...20	20...21	21...22	*4...16*
40	1.2 %	0.6 %	1.3 %	-0.6 %	-1.1 %	-0.8 %	0.0 %	-0.9 %	-1.1 %	-0.9 %	-1.1 %	-0.6 %	-0.5 %	0.3 %	1.8 %	0.5 %	1.7 %	-1.0 %	-1.5 %		**-0.1 %**
60	2.4 %	0.7 %	1.4 %	0.6 %	-0.3 %	-0.5 %	0.3 %	0.3 %	0.2 %	-0.1 %	0.0 %	-0.3 %	-0.3 %	1.0 %	1.0 %	1.7 %	1.7 %	1.8 %	2.8 %		**0.8 %**
80	3.7 %	1.5 %	2.1 %	0.9 %	0.1 %	-0.8 %	0.2 %	1.4 %	0.5 %	-0.1 %	0.4 %	-0.2 %	-0.5 %	0.6 %	0.7 %	0.1 %	1.4 %	2.0 %	1.8 %	3.5 %	**1.0 %**
100	1.3 %	1.9 %	1.5 %	1.2 %	-0.2 %	0.5 %	0.6 %	0.7 %	0.7 %	0.5 %	1.0 %	0.4 %	0.0 %	1.4 %	0.3 %	0.9 %	1.5 %	1.6 %	2.2 %	2.0 %	**1.0 %**
120	1.1 %	2.6 %	1.1 %	1.3 %	-0.1 %	2.1 %	0.6 %	0.8 %	0.8 %	0.6 %	0.7 %	0.9 %	-1.1 %	1.2 %	0.6 %	1.4 %	0.6 %	2.3 %	1.6 %	2.2 %	**1.1 %**
140	0.6 %	1.2 %	1.2 %	0.9 %	0.7 %	-0.9 %	0.3 %	1.5 %	0.5 %	0.7 %	1.1 %	2.4 %	-0.5 %	1.5 %	0.7 %	1.8 %	0.8 %	1.7 %	2.7 %	1.7 %	**1.0 %**
160	-0.3 %	4.3 %	-1.2 %	1.8 %	1.0 %	-0.3 %	0.5 %	1.1 %	0.6 %	0.8 %	2.5 %	1.6 %	5.5 %	1.9 %	2.0 %	1.2 %	1.2 %	1.5 %	2.5 %	3.2 %	**1.6 %**
180	1.3 %	0.5 %	2.6 %	0.0 %	0.4 %	0.0 %	-0.7 %	0.9 %	1.5 %	0.9 %	2.1 %	2.1 %	2.7 %	1.1 %	0.5 %	0.9 %	1.8 %	1.0 %	1.8 %	1.6 %	**1.1 %**
200	2.0 %	-1.8 %	1.8 %	3.2 %	0.4 %	-1.2 %	0.5 %	0.7 %	0.5 %	1.3 %	1.6 %	1.6 %	3.4 %	1.6 %	0.7 %	2.0 %	1.7 %	1.8 %	1.5 %	1.3 %	**1.2 %**
250	6.1 %	-4.2 %	-1.6 %	-0.6 %	1.5 %	-1.8 %	1.1 %	-1.6 %	0.9 %	0.1 %	0.1 %	0.2 %	1.2 %	-1.3 %	5.1 %	0.9 %	1.3 %	1.0 %	2.5 %	-6.4 %	**0.2 %**
...	**1.9 %**	**0.7 %**	**1.0 %**	**0.9 %**	**0.2 %**	**-0.4 %**	**0.3 %**	**0.5 %**	**0.5 %**	**0.4 %**	**0.8 %**	**0.8 %**	**1.0 %**	**0.9 %**	**1.3 %**	**1.1 %**	**1.4 %**	**1.4 %**	**1.8 %**	**1.1 %**	**0.7 %**

Root Mean Square Error (RMSE)

Height	Velocity bin [m/s]																				
[m]	2...3	3...4	4...5	5...6	6...7	7...8	8...9	9...10	10...11	11...12	12...13	13...14	14...15	15...16	16...17	17...18	18...19	19...20	20...21	21...22	*4...16*
40	5.6 %	4.1 %	3.2 %	3.2 %	3.0 %	3.0 %	3.1 %	3.2 %	2.9 %	3.4 %	3.2 %	3.0 %	3.6 %	3.1 %	2.5 %	1.7 %	2.1 %	2.4 %	4.3 %		**3.2 %**
60	5.1 %	4.0 %	3.1 %	2.7 %	3.1 %	2.5 %	2.9 %	2.9 %	2.7 %	2.8 %	2.8 %	2.6 %	3.1 %	3.4 %	2.6 %	2.4 %	2.4 %	2.7 %	2.5 %		**3.0 %**
80	4.7 %	4.0 %	3.3 %	2.8 %	2.7 %	2.8 %	2.8 %	3.3 %	3.0 %	2.8 %	2.4 %	2.6 %	2.4 %	2.4 %	2.5 %	1.9 %	2.5 %	2.6 %	2.3 %	3.0 %	**2.8 %**
100	4.5 %	3.8 %	3.8 %	2.8 %	2.4 %	3.9 %	2.6 %	2.9 %	2.7 %	2.8 %	2.8 %	2.8 %	2.7 %	2.5 %	2.1 %	1.9 %	2.4 %	2.1 %	2.3 %	2.1 %	**2.8 %**
120	5.1 %	5.6 %	3.8 %	2.8 %	2.6 %	5.5 %	3.2 %	3.3 %	2.7 %	2.7 %	2.7 %	2.6 %	2.6 %	2.2 %	2.4 %	2.3 %	1.9 %	2.5 %	2.2 %	2.2 %	**3.0 %**
140	4.5 %	4.3 %	3.8 %	4.5 %	2.7 %	2.8 %	3.0 %	4.5 %	2.6 %	3.0 %	2.5 %	3.0 %	2.6 %	2.4 %	2.3 %	2.0 %	1.7 %	2.4 %	2.4 %	2.3 %	**3.0 %**
160	4.8 %	7.4 %	5.1 %	5.3 %	3.0 %	2.7 %	3.6 %	4.0 %	2.5 %	2.7 %	4.4 %	3.2 %	5.7 %	2.3 %	2.7 %	1.8 %	2.3 %	2.3 %	2.5 %	2.8 %	**3.6 %**
180	4.5 %	4.9 %	4.8 %	5.1 %	3.0 %	3.7 %	4.6 %	4.1 %	3.3 %	2.6 %	4.1 %	2.9 %	3.3 %	2.1 %	1.9 %	1.6 %	2.3 %	2.0 %	2.1 %	2.2 %	**3.3 %**
200	5.4 %	4.6 %	5.9 %	5.6 %	2.9 %	2.8 %	3.4 %	3.6 %	4.8 %	2.8 %	3.1 %	3.2 %	3.9 %	2.3 %	2.4 %	2.8 %	2.5 %	1.9 %	2.2 %	1.9 %	**3.4 %**
250	8.0 %	7.0 %	8.3 %	5.0 %	4.9 %	3.9 %	4.5 %	3.8 %	4.0 %	2.7 %	3.4 %	2.6 %	3.4 %	3.0 %	5.5 %	2.3 %	2.4 %	2.5 %	2.7 %	7.9 %	**4.4 %**
...	**5.2 %**	**5.0 %**	**4.5 %**	**4.0 %**	**3.0 %**	**3.4 %**	**3.4 %**	**3.6 %**	**3.1 %**	**2.8 %**	**3.2 %**	**2.9 %**	**3.3 %**	**2.6 %**	**2.7 %**	**2.1 %**	**2.2 %**	**2.3 %**	**2.5 %**	**3.1 %**	**3.3 %**

Table A.1: Aggregated TI error numbers for MBE, representative TI and RMSE of compensated FLS for WS199 at Frøya.

Aggregated TI data

Mean bias error (MBE)

Height [m]	Velocity bin [m/s] 2...3	3...4	4...5	5...6	6...7	7...8	8...9	9...10	10...11	11...12	12...13	13...14	14...15	15...16	16...17	17...18	18...19	19...20	20...21	21...22	*4...16*
40	3.5 %	1.2 %	0.6 %	0.5 %	-0.3 %	-0.2 %	0.4 %	-0.3 %	-0.9 %	-0.5 %	-1.4 %	-0.7 %	-1.6 %	-0.8 %	-0.6 %	0.2 %	-0.2 %	0.1 %	-0.4 %		-0.1 %
60	2.7 %	1.5 %	1.3 %	0.7 %	0.7 %	0.2 %	0.8 %	0.7 %	0.4 %	0.2 %	-0.3 %	-0.1 %	-0.7 %	0.6 %	-0.1 %	-0.2 %	0.5 %	-0.3 %	1.5 %		0.5 %
80	2.8 %	1.6 %	1.1 %	0.8 %	1.0 %	0.4 %	1.1 %	1.2 %	0.8 %	0.4 %	0.8 %	0.1 %	0.1 %	0.1 %	0.5 %	0.2 %	0.6 %	0.9 %	0.7 %	2.0 %	0.9 %
100	2.5 %	1.7 %	1.3 %	0.8 %	0.9 %	0.7 %	1.2 %	1.4 %	1.2 %	0.5 %	1.2 %	0.8 %	0.8 %	1.2 %	0.7 %	0.5 %	0.6 %	0.7 %	1.1 %	1.4 %	1.1 %
120	2.4 %	2.3 %	2.1 %	1.4 %	0.8 %	0.4 %	1.4 %	1.4 %	1.1 %	1.0 %	1.1 %	0.7 %	0.4 %	0.4 %	0.9 %	0.5 %	1.6 %	0.2 %	1.4 %	0.0 %	1.1 %
140	3.0 %	1.4 %	1.9 %	0.9 %	0.9 %	0.3 %	1.1 %	1.9 %	1.1 %	1.4 %	1.3 %	1.1 %	0.6 %	0.6 %	1.1 %	0.5 %	0.7 %	0.7 %	1.0 %	0.5 %	1.1 %
160	2.6 %	2.1 %	1.1 %	0.6 %	1.2 %	0.3 %	1.2 %	1.7 %	1.2 %	0.6 %	1.7 %	1.4 %	1.8 %	1.1 %	1.0 %	0.6 %	-0.2 %	-0.1 %	1.5 %	1.2 %	1.1 %
180	2.6 %	1.3 %	1.8 %	1.3 %	0.9 %	0.2 %	1.0 %	1.4 %	1.0 %	1.1 %	1.4 %	1.2 %	1.3 %	0.8 %	1.0 %	0.8 %	-0.1 %	0.3 %	1.0 %	1.3 %	1.1 %
200	3.1 %	1.0 %	2.5 %	1.6 %	1.1 %	0.6 %	1.0 %	1.8 %	1.3 %	1.0 %	0.9 %	1.6 %	1.4 %	0.9 %	0.9 %	1.3 %	0.7 %	0.6 %	0.7 %	1.1 %	1.3 %
250	2.0 %	1.3 %	1.1 %	1.4 %	0.4 %	-0.2 %	0.9 %	0.6 %	1.6 %	0.7 %	0.1 %	1.2 %	1.5 %	0.1 %	1.8 %	0.6 %	0.6 %	0.0 %	0.3 %	-0.5 %	0.8 %
...	**2.7 %**	**1.5 %**	**1.5 %**	**1.0 %**	**0.8 %**	**0.3 %**	**1.0 %**	**1.2 %**	**0.9 %**	**0.6 %**	**0.7 %**	**0.7 %**	**0.6 %**	**0.5 %**	**0.7 %**	**0.5 %**	**0.5 %**	**0.3 %**	**0.9 %**	**0.9 %**	**0.9 %**

Representative TI error

Height [m]	Velocity bin [m/s] 2...3	3...4	4...5	5...6	6...7	7...8	8...9	9...10	10...11	11...12	12...13	13...14	14...15	15...16	16...17	17...18	18...19	19...20	20...21	21...22	*4...16*
40	4.1 %	0.2 %	0.8 %	-0.7 %	-1.7 %	-1.0 %	0.0 %	-0.8 %	-1.3 %	-1.3 %	-1.4 %	-0.3 %	-2.0 %	-1.3 %	-0.4 %	2.1 %	0.7 %	0.6 %	-1.4 %		-0.3 %
60	3.1 %	0.5 %	1.3 %	0.7 %	-0.3 %	-0.6 %	0.2 %	-0.1 %	-0.4 %	-0.1 %	0.1 %	-0.9 %	-1.2 %	1.4 %	0.4 %	0.1 %	0.9 %	0.2 %	3.1 %		0.4 %
80	3.8 %	0.8 %	1.0 %	0.7 %	0.3 %	-1.1 %	0.3 %	1.0 %	0.4 %	0.0 %	1.8 %	-0.2 %	-0.2 %	1.0 %	1.0 %	1.0 %	0.9 %	1.7 %	2.1 %	2.2 %	0.9 %
100	2.1 %	1.5 %	3.8 %	0.4 %	0.4 %	-0.2 %	0.4 %	1.2 %	0.8 %	0.0 %	1.7 %	1.4 %	0.1 %	1.4 %	1.8 %	0.7 %	1.3 %	1.2 %	1.3 %	2.1 %	1.2 %
120	1.7 %	6.5 %	4.9 %	2.0 %	0.2 %	0.1 %	1.2 %	0.9 %	0.1 %	0.5 %	0.9 %	1.1 %	-0.3 %	1.0 %	2.1 %	0.6 %	2.8 %	0.7 %	2.5 %	0.6 %	1.5 %
140	2.8 %	1.0 %	2.2 %	0.3 %	0.8 %	-0.8 %	0.3 %	1.8 %	1.1 %	0.8 %	1.6 %	2.8 %	-0.1 %	1.2 %	2.9 %	0.9 %	1.8 %	1.9 %	2.5 %	1.5 %	1.4 %
160	3.5 %	3.2 %	-1.0 %	-0.5 %	1.0 %	-0.9 %	0.7 %	1.7 %	1.2 %	-0.2 %	3.3 %	1.7 %	5.6 %	1.8 %	2.4 %	1.0 %	-0.2 %	0.1 %	3.3 %	2.1 %	1.5 %
180	1.4 %	0.0 %	4.0 %	0.7 %	0.7 %	-1.7 %	-1.7 %	0.9 %	0.8 %	1.0 %	2.8 %	0.9 %	4.2 %	1.3 %	1.3 %	1.5 %	0.5 %	0.1 %	1.5 %	2.1 %	1.1 %
200	1.9 %	-1.2 %	5.5 %	2.4 %	0.8 %	-0.9 %	0.1 %	1.4 %	-0.5 %	0.3 %	1.0 %	1.9 %	4.7 %	1.7 %	1.2 %	1.6 %	2.9 %	0.8 %	1.8 %	2.2 %	1.5 %
250	1.0 %	-3.1 %	-1.6 %	1.1 %	-1.6 %	-2.8 %	0.4 %	-1.2 %	0.8 %	-0.4 %	-1.6 %	0.7 %	1.6 %	-2.1 %	7.9 %	0.3 %	0.5 %	-0.4 %	0.5 %	-6.6 %	-0.3 %
...	**2.5 %**	**0.9 %**	**2.1 %**	**0.7 %**	**0.1 %**	**-1.0 %**	**0.2 %**	**0.7 %**	**0.3 %**	**0.1 %**	**1.0 %**	**0.9 %**	**1.2 %**	**0.7 %**	**2.1 %**	**1.0 %**	**1.2 %**	**0.7 %**	**1.7 %**	**0.8 %**	**0.8 %**

Root Mean Square Error (RMSE)

Height [m]	Velocity bin [m/s] 2...3	3...4	4...5	5...6	6...7	7...8	8...9	9...10	10...11	11...12	12...13	13...14	14...15	15...16	16...17	17...18	18...19	19...20	20...21	21...22	*4...16*
40	5.9 %	3.9 %	3.2 %	3.7 %	3.9 %	3.4 %	2.9 %	3.4 %	3.5 %	3.3 %	3.5 %	3.5 %	3.0 %	2.6 %	2.0 %	2.5 %	2.1 %	2.2 %	1.2 %		3.1 %
60	5.2 %	4.6 %	3.2 %	3.2 %	3.2 %	3.6 %	3.4 %	3.0 %	2.8 %	3.2 %	2.6 %	2.8 %	3.2 %	2.7 %	2.5 %	2.2 %	2.3 %	2.2 %	2.4 %		3.1 %
80	5.6 %	4.1 %	3.3 %	2.9 %	3.2 %	3.4 %	3.5 %	3.5 %	2.8 %	2.8 %	2.9 %	2.8 %	3.2 %	3.1 %	2.2 %	2.2 %	2.6 %	2.3 %	2.1 %	2.4 %	3.0 %
100	4.6 %	4.5 %	6.3 %	2.6 %	3.6 %	3.6 %	3.2 %	3.6 %	2.9 %	2.4 %	2.5 %	2.8 %	2.5 %	2.5 %	2.7 %	1.9 %	2.5 %	2.2 %	2.2 %	2.3 %	3.1 %
120	5.4 %	7.8 %	6.3 %	3.9 %	3.0 %	4.3 %	4.4 %	3.3 %	2.8 %	2.8 %	2.6 %	2.4 %	2.3 %	2.6 %	2.6 %	2.0 %	2.9 %	2.0 %	2.8 %	2.0 %	3.4 %
140	5.8 %	4.2 %	5.0 %	4.5 %	3.3 %	4.1 %	3.3 %	4.2 %	3.3 %	3.0 %	2.8 %	3.0 %	2.7 %	2.2 %	2.8 %	2.2 %	2.3 %	2.2 %	2.4 %	2.2 %	3.3 %
160	6.1 %	5.9 %	5.0 %	4.5 %	3.4 %	2.9 %	3.8 %	4.6 %	3.2 %	2.5 %	4.6 %	2.9 %	5.5 %	2.9 %	2.4 %	2.1 %	1.5 %	2.0 %	2.8 %	2.4 %	3.5 %
180	5.1 %	4.6 %	6.1 %	6.2 %	3.3 %	3.5 %	4.7 %	4.1 %	3.1 %	2.9 %	3.9 %	3.2 %	3.7 %	2.5 %	2.1 %	2.4 %	1.8 %	1.9 %	2.2 %	2.8 %	3.5 %
200	5.6 %	4.7 %	7.1 %	5.4 %	3.3 %	3.9 %	3.1 %	4.1 %	5.4 %	2.7 %	2.9 %	3.2 %	4.4 %	2.6 %	2.6 %	2.5 %	3.2 %	2.4 %	2.6 %	2.3 %	3.7 %
250	4.9 %	6.2 %	8.6 %	8.1 %	5.3 %	3.8 %	4.7 %	3.9 %	4.3 %	2.8 %	4.6 %	3.0 %	3.7 %	3.6 %	6.8 %	2.1 %	2.5 %	1.7 %	2.3 %	8.0 %	4.5 %
...	**5.4 %**	**5.0 %**	**5.4 %**	**4.5 %**	**3.5 %**	**3.6 %**	**3.7 %**	**3.8 %**	**3.4 %**	**2.8 %**	**3.3 %**	**3.0 %**	**3.4 %**	**2.7 %**	**2.9 %**	**2.2 %**	**2.4 %**	**2.1 %**	**2.3 %**	**3.1 %**	**3.6 %**

Table A.2: Aggregated TI error numbers for MBE, representative TI and RMSE of compensated FLS for SWLB044 at Frøya.